HOSTED BY

ELSEVIER

CrossMark

Available online at www.sciencedirect.com

ScienceDirect

Progress in Natural Science: Materials International 25 (2015) 379–385

Progress in Natural Science Materials International

www.elsevier.com/locate/pnsmi
www.sciencedirect.com

Original Research

Influence of graphene microstructures on electrochemical performance for supercapacitors

Youning Gong[a], Delong Li[a], Qiang Fu[a,b], Chunxu Pan[a,b,*]

[a]School of Physics and Technology, and MOE Key Laboratory of Artificial Micro- and Nano-structures, Wuhan University, Wuhan 430072, China
[b]Shenzhen Research Institute, Wuhan University, Shenzhen 518057, China

Received 6 April 2015; accepted 19 June 2015
Available online 10 November 2015

Abstract

The influence of variant graphenes on electrochemical performance for supercapacitors was studied comparatively and systematically by using SEM, FTIR and Raman spectroscopy, cyclic voltammetry (CV), galvanostatic charge/discharge and electrochemical impedance spectroscopy (EIS). The results revealed that: 1) the nitrogen-doped graphene (N-G) electrode exhibited the highest specific capacitance at the same voltage scan rate; 2) the specific capacitance of the N-G reached up to 243.5 F/g at 1 A/g, while regular graphite oxide (GO) was 43.5 F/g and reduced graphene oxide (rGO) was 67.9 F/g; 3) N-G exhibited the best supercapacitance performance and the superior electrochemical properties, which made it an ideal electrode material for supercapacitors.
© 2015 Chinese Materials Research Society. Production and hosting by Elsevier B.V. This is an open access article under the CC BY-NC-ND license (http://creativecommons.org/licenses/by-nc-nd/4.0/).

Keywords: Graphene; Nitrogen doping; Microstructure; Supercapacitor

1. Introduction

As a new type of energy storage devices, supercapacitors exhibit both high capacitance and large energy density, which bridge the gap between conventional capacitors and rechargeable batteries, and have advantages in applications, such as electronic communication, transportation, aerospace and other fields [1–3]. Electrode materials are the key component of supercapacitor, and determine its main performance parameters [4–7]. Recently, graphene, a new carbon material with one-atom thick layer 2D structure, has been recognized as an ideal material for electrochemical energy storage, due to its unique properties of high electrical conductivity, large surface area, and chemical stability, etc. [8–12].

Some researches have been reported about the graphene-based supercapacitors. Rao and his co-workers [13] prepared graphene by three methods and compared their capacitive behaviors. With aq. H_2SO_4 as the electrolyte, the specific capacitance of samples prepared by exfoliation of graphite oxide reached up to 117 F/g, while samples prepared by transformation of nano-diamond and the decomposition of camphor had lower values as 35 F/g and 6 F/g. Stoller et al. [14] synthesized chemical modified graphene by reducing graphene oxide sheets with hydrazine hydrate, and its specific capacitances were 135 F/g and 99 F/g in aqueous and organic electrolytes respectively. Chen et al. [15] fabricated the graphene with few layers by using hydrobromic acid as reductant, and the maximum specific capacitance reached to 348 F/g, which was the highest value of the chemical modified graphene so far. Jeong et al. [16] developed supercapacitors based on nitrogen-doped graphene, which exhibited a specific capacitance up to 280 F/g, i.e. about 4 times higher than that of pristine graphene. Thus it can be seen that the graphene sheets with different types or microstructures have great influences on the performance of supercapacitors.

In this paper, variant graphenes involving graphite oxide (GO), reduced graphene oxide (rGO) and nitrogen-doped graphene (N-G) were prepared and their microstructures have been characterized. Then these graphenes were fabricated as electrode materials of

*Corresponding author at: School of Physics and Technology, Wuhan University, Wuhan 430072, China. Tel.: +86 27 68752481x8168.
E-mail address: cxpan@whu.edu.cn (C. Pan).
Peer review under responsibility of Chinese Materials Research Society.

http://dx.doi.org/10.1016/j.pnsc.2015.10.004
1002-0071/© 2015 Chinese Materials Research Society. Production and hosting by Elsevier B.V. This is an open access article under the CC BY-NC-ND license (http://creativecommons.org/licenses/by-nc-nd/4.0/).

supercapacitors. For comparisons, their electrochemical properties including cyclic voltammetry (CV), galvanostatic charge/discharge and electrochemical impedance spectroscopy (EIS) were measured under the same experimental conditions. Clearly, the influences of the different graphene microstructures on electrochemical performance for supercapacitors were deeply revealed, and it is expected to provide the theoretical and experimental basis for further study on graphene-based energy storage devices.

2. Experimental

2.1. Preparation of graphite oxide

Graphite oxide (GO) was synthesized from natural graphite powders by a modified Hummers method [17] including following steps : 1) A pretreatment was used to obtain GO with fully oxidation and less impurities, i.e., graphite powder (1.0 g), $K_2S_2O_4$ (0.5 g) and P_2O_5 (0.5 g) were mixed into concentrated H_2SO_4 (2–4 mL), and the mixture was continually stirred in 80 °C water bath for 6 h, and then the product was filtrated by deionized water for several times and dried at 60 °C. 2) The pre-oxidized graphite was dispersed into 30 mL 98% H_2SO_4, and then 4 g $KMnO_4$ was slowly added while stirring and cooling with ice-water bath. 3) The solution was transferred into 35 °C water bath. 4) 30 mL deionized water was added into the solution after 2 h, and maintained in the temperature range of 80–90 °C for 1 h. After that, 30% H_2O_2 solution was added until the color of the suspension turned to bright yellow. 5) The GO was finally obtained after pickling, washing, filtration and drying.

2.2. Preparations of graphene and N-doped graphene

2.2.1. Preparations of graphene

1) 0.5 g of the prepared GO was dispersed into 1 L deionized water with the aid of ultrasonication to obtain 0.5 mg/mL GO dispersion. 2) 30 mL of the dispersion was put into a Teflon lined stainless-steel autoclave, and then the autoclave was sealed and maintained at 180 °C for 3 h in an electric oven. 3) The product was collected and washed with deionized water for several times, followed by drying at 80 °C to obtain reduced GO.

2.2.2. Preparations of N-doped graphene (N-G)

1) Taking out 30 mL of the prepared GO dispersion and adding the ammonium hydroxide as the nitrogen dopant. 2) After stirring for 30 min, the resultant mixture was transferred into a Teflon lined stainless-steel autoclave, and treated under the same experimental conditions as above. 3) Finally, the black product was collected and washed with deionized water for several times, followed by drying at 80 °C to obtain N-G.

2.3. Characterizations

The microstructures and morphologies of the samples were characterized by using the following facilities of scanning electron microscope (SEM, S-4800, Hitachi, Japan); transmission electron microscope (TEM, JEM-2010, JEOL, Japan); X-ray photoelectron spectroscope (XPS, ESCALAB 250Xi, Thermo Fisher Scientific, USA) with Al Kα radiation of 1486.6 eV as the excitation source; Fourier transform infrared (FTIR) spectrometer with scanning range of 400–4000 cm^{-1} (FT-IR, Nicolet iS10, Thermo fisher, USA) and laser scanning confocal micro-Raman spectrometer (LabRAM HR, HORIBA, France) with a laser excitation wavelength 488 nm and scans on an extended range (1000–3000 cm^{-1}).

2.4. Electrode preparation and electrochemical measurements

2.4.1. Electrode preparation

Nickel foam was used as the current collector, and electrode materials were GO, rGO and N-G. The preparation process was as follows: 1) Nickel foam was cut into rectangle sheets (20 mm*10 mm); 2) the mixture containing 80 wt% active material, 10 wt% conductive carbon black and 10 wt% PVDF was well mixed with appropriate amount of N-methyl-2-pyrrolidone (NMP), and grinded for 1 h to obtain the dark paste; 3) the paste was casted on nickel foam and dried in a vacuum oven at 80 °C for 12 h; 4) finally, the electrode was obtained by pressing at 10 MPa for 1 min. The mass of active materials on each working electrode was about 1.5 mg.

2.4.2. Electrochemical measurements

All the experimental measurements were carried out in a three-electrode system, in which the nickel foam as working electrode, platinum as counterelectrode, and saturated calomel electrode (SCE) as reference electrode, and 6 M KOH was used as aqueous electrolyte solution. The electrochemical performances involving cyclic voltammetry (CV), galvanostatic charge/discharge and electrochemical impedance spectroscopy (EIS) were measured by using the Electrochemical Working Station (CHI660D, Shanghai Chenhua, China). The cyclic voltammetry (CV) was recorded with a voltage range from −0.1 V to −1.1 V, and the electrochemical impedance spectroscopy (EIS) was recorded in the frequency range of 0.1–100,000 Hz by applying an AC voltage with 5 mV perturbation.

3. Results and discussion

3.1. Microstructures characterizations of graphenes

Fig. 1 shows the SEM and TEM images of the GO, rGO and N-G. Clearly, graphite oxide (GO) showed single or a few layer microstructure with wrinkles and defects on the surface, which may be due to large amount of functional groups, such as hydroxyl, carboxyl on the edge, and carboxyl and epoxide groups in the inner part. These groups expanded the interlayer distance of graphite, and destroyed its integrated layer microstructure, which resulted in the wrinkle phenomenon. However, the reduced graphene oxide (rGO) presented a different morphology as fluffy and transparent layers with rich wrinkles and fluctuation. The fluctuation was essential to sustain the thermodynamic stability of graphene, due to its 2D crystal structure. These disordered graphene sheets could connect as a 3D porous network, which was conducive to the contact of electrolyte and electrode materials. Comparing to regular graphene, the nitrogen-doped graphene (N-G) exhibits the similar microstructure, such as, fluffy

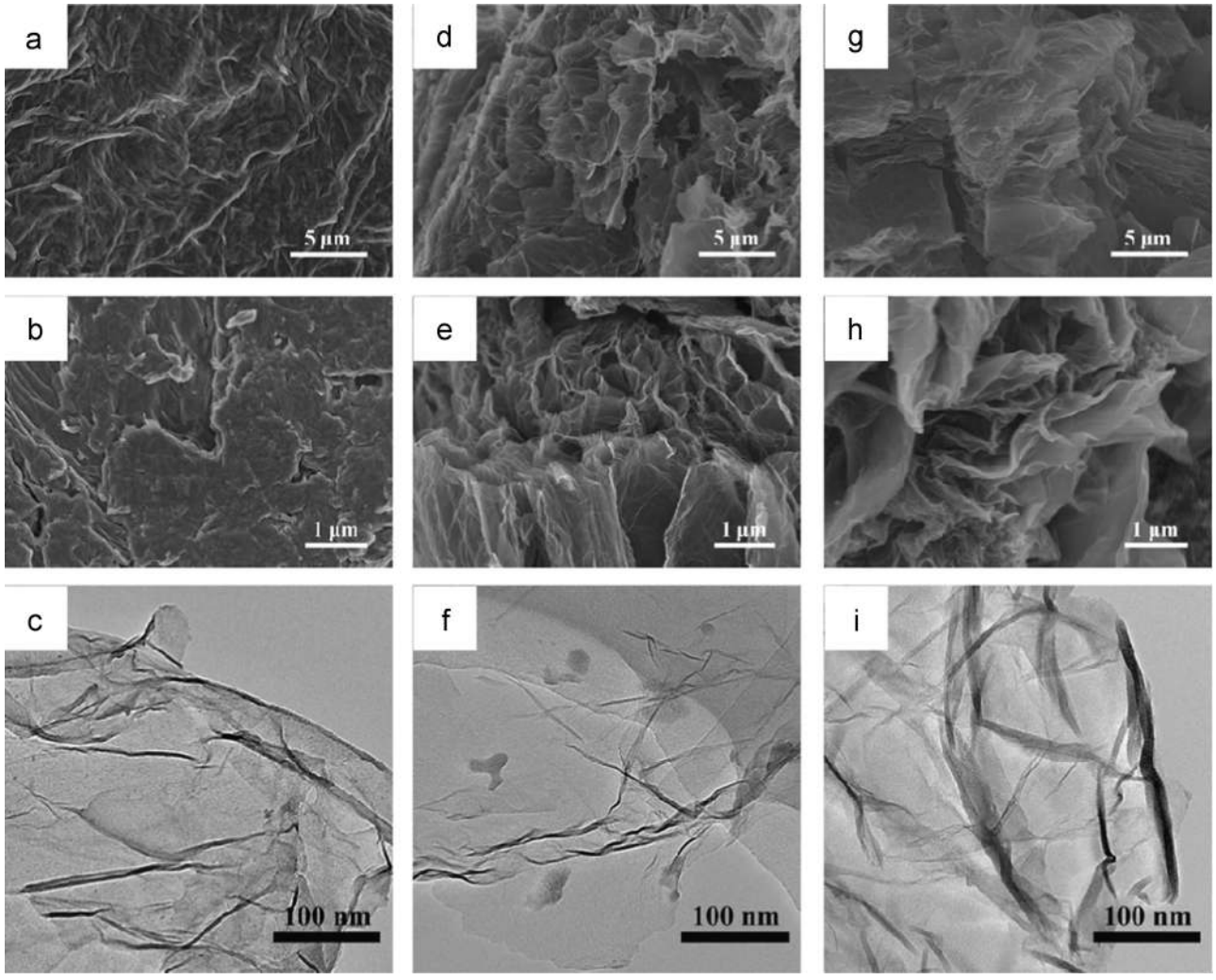

Fig. 1. SEM and TEM images of different graphenes. SEM images: (a) and (b) GO; (d) and (e) rGO; (g) and (h) N-G. (top: low magnification, middle: high magnification). TEM images: (c) GO; (f) rGO; (i) N-G.

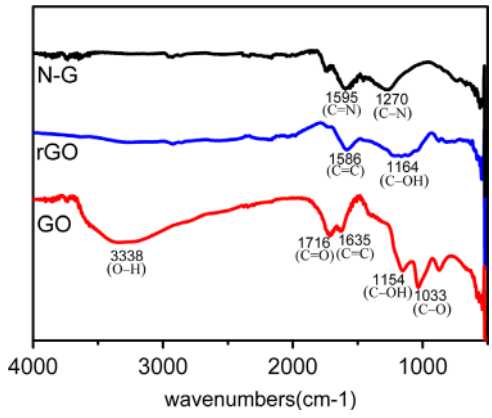

Fig. 2. FTIR spectra of GO, rGO and N-G.

and transparent layers, wrinkles at the edge, but more aggregations, as shown in Fig. 1(g)–(i).

3.2. FTIR spectra of graphenes

Fig. 2 illustrates the FTIR spectra of GO, rGO and N-G. Obviously, the spectrum of GO showed: 1) a broad band at 3338 cm^{-1}, which belongs to a strong stretching mode of OH group; 2) an absorption peak at 1635 cm^{-1} due to C=C stretching mode; 3) the peaks at 1716, 1154 and 1033 cm^{-1}, which correspond to the stretching modes of C=O, C–OH and C–O, respectively. However, for rGO, the absorption peak in the 3338 cm^{-1} region disappeared, which reveals the absence of OH group after reduction. And the peak at 1586 cm^{-1} belongs to C=C, while the absorption peak at 1164 cm^{-1} still existed, which is attributed to C–OH. These results indicated that the partial functional groups in GO had been effectively eliminated during hydrothermal treatment. Furthermore for the N-G, the disappeared absorption peak of oxygenous groups demonstrated that GO had been effectively reduced by hydrothermal treatment. And two new absorption peaks appeared at 1595 and 1270 cm^{-1}, which may be attributed to the bands of C=N and C–N, i.e., the graphene was successfully N-doped.

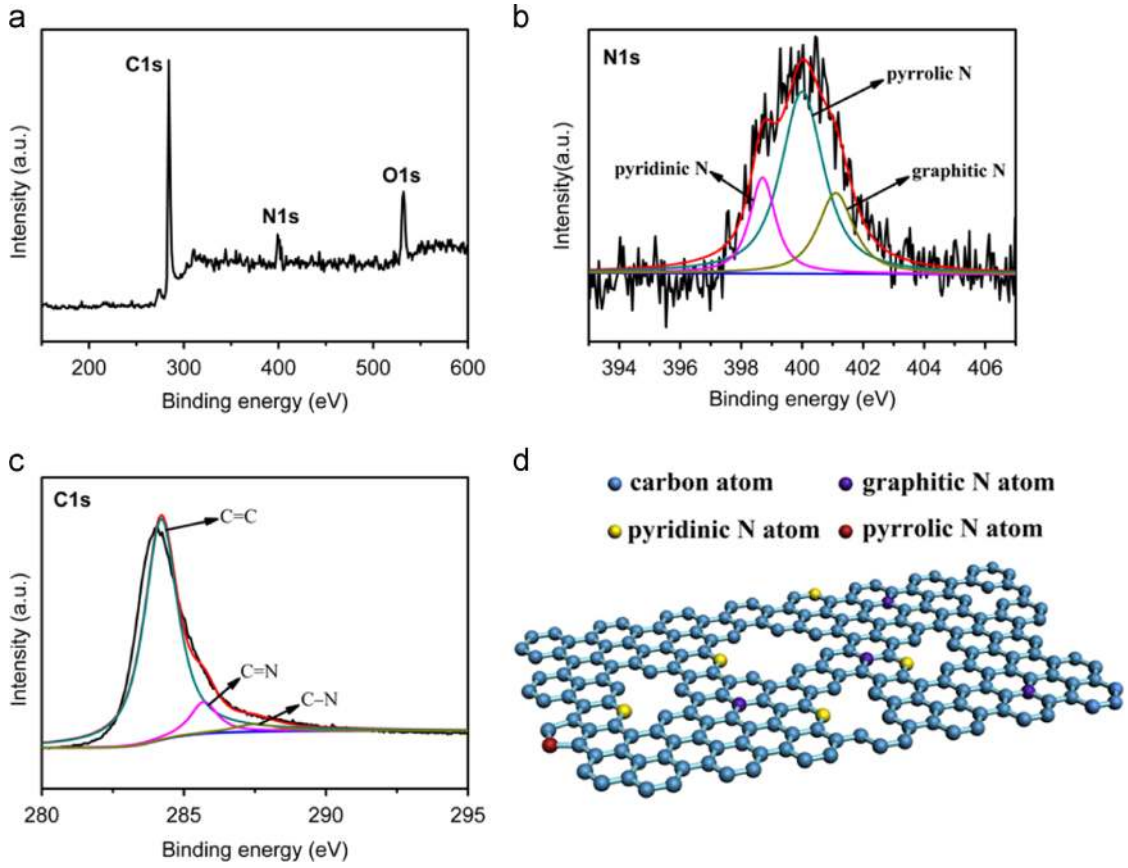

Fig. 3. (a) XPS wide spectra, (b) high-resolution N1s XPS spectra and (c) high-resolution C1s XPS spectra of N-G; (d) bonding configurations for nitrogen atoms in N-G.

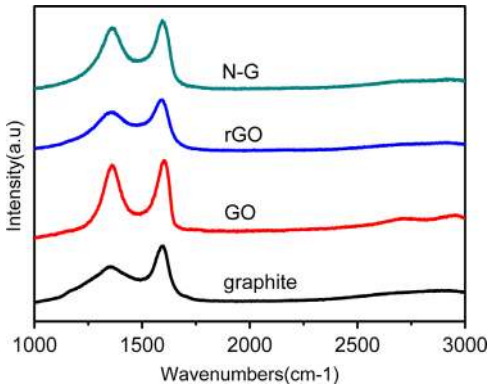

Fig. 4. Raman spectra of graphite, GO, rGO and N-G.

3.3. XPS spectra of N-doped graphene

XPS is an effective technique for surface chemical analysis to determine the species and chemical states of elements in the surface of materials. Fig.3 illustrates the XPS spectra of the N-G sample. It was found that N-G exhibited three peaks, i.e., a predominant C1s peak at ~284.2 eV, O1s peak at ~532.0 eV and an obvious N1s peak at ~399.9 eV. From analysis of the XPS spectra, the N content in the N-G sample was about 3.77 wt%. For peak fittings, the C1s and N1s background spectra were removed by using Shirley algorithm. In general, when a nitrogen atom is doped into graphene, there are three bonding configurations within the carbon lattice, that is, graphitic N (~401.1 eV), pyrrolic N (~399.9 eV) and pyridinic N (~398.7 eV), as shown in Figs. 3(b) and (d) [18]. Therefore it was confirmed that N atoms have been doped into the graphene lattice successfully, and the pyrrolic N occupied the dominant portion. In addition, the C1s spectrum (Fig. 3(c)) could be divided into three individual peaks, i.e., the sharp peak at ~284.2 eV corresponding to C=C bonds, and peaks at ~285.7 eV and ~287.5 eV assigned to C=N and C–N [18].

3.4. Raman spectra of graphenes

Raman spectroscopy is a very important instrument to characterize carbon materials because Raman scattering is of close relationship with electron structure of the substances. Fig. 4 illustrates the Raman spectra of graphite, GO, rGO and N-G. It is well-known that the G peak at 1580 cm^{-1} is the characteristic peak of sp^2 hybrid structure, which represents the symmetry and crystallizability of carbon materials; and the D peak at 1350 cm^{-1} is the defect peak, which represents the surface defect and disorder of graphite layers. In general, the intensity ratio of I_D/I_G is used to characterize the order or disorder degree of carbon materials, i.e., the higher the I_D/I_G, the larger disorder degree of the carbon materials [19,20]. According to the spectra, we got the following results: 1) compared to graphite ($I_D/I_G=0.64$), the value of GO $I_D/I_G=0.92$ indicated that the chemical treatment destroyed the integrated layers and introduced large amount of defects on the

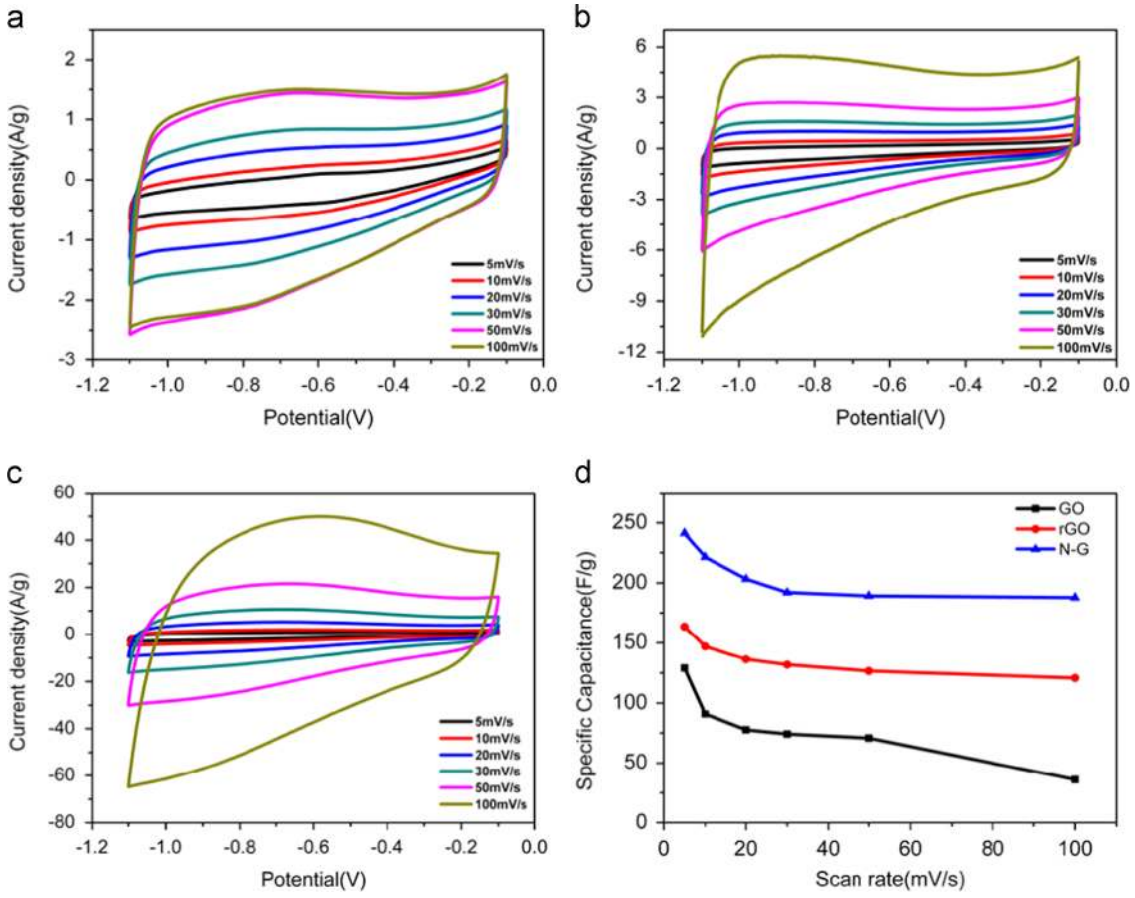

Fig. 5. CV curves of samples. (a) GO, (b) rGO, (c) N-G; (d) Specific capacitances of GO, rGO and N-G at different scan rates.

surface of graphite; 2) the value of rGO $I_D/I_G=0.78$ revealed that the reduction treatment wiped off the oxygenous groups and restored its original layer structure; 3) due to the introduction of N atoms, the substitution of N dopants disordered the graphene lattice integrity, and thus more surface defects exist in N-G ($I_D/I_G=0.88$) than rGO.

3.5. Cyclic voltammetry

In order to investigate the electrochemical properties as supercapacitor, the graphene samples GO, rGO, and N-G were prepared as the electrode materials. Fig. 5(a)–(c) gives the CV curves of three electrodes at a series of scan rates (5, 10, 20, 30, 50, and 100 mV/s) with a voltage range from −0.1 V to −1.1 V. It was found that the shapes of all CV curves were approximately rectangular and exhibited a good symmetry, even at a high scan rate, which demonstrated an excellent capacitive behavior and rate performance. At the low scan rate, the speed of charge and discharge was relatively slow, which allowed the ions in electrolyte to have enough time to diffuse into graphene layers, and therefore, the electrodes exhibited a higher specific capacitance. However, at a high scan rate the process of charge and discharge was too quick for the full ion diffusion, and the less utilization of electrode surface resulted in a lower specific capacitance. During scanning no redox peak existed in the CV curves, which indicated that the electrodes were of excellent electrochemical stability [21].

The specific capacitance (C) was calculated according to the equation

$$C=\frac{\int_0^{2V_0/v}|i|dt}{2mV_0}$$

where v is the scan rate, V_0 is the voltage difference, i is the current, and m is the mass of active materials [22]. According to Fig. 5(d), the N-G electrode possessed the highest specific capacitance at the same scan rates. These may be ascribed to following reasons: 1) the porous microstructure of N-G enhanced the electrode/electrolyte wettability and contributed to form an electric double layer capacitor; 2) under hydrothermal condition, the N-G conductivity increased greatly, which accelerated the electron mobility on the surface of electrode; [23,24] 3) the N-doping into graphene lattice could increase the binding energy, which led to more accommodations for the ions on a certain surface area of electrode, and exhibited further higher capacitance [16].

3.6. Galvanostatic charge/discharge

Fig. 6(a–b–c) shows the galvanostatic charge/discharge curves of GO, rGO and N-G at a series of current densities (1.0, 2.0, 3.0, 5.0, and 10.0 A/g) with a voltage range from −0.1 V to −1.1 V. Obviously, three curves were linear in the range of voltage with constant slopes, which indicated the ideal double layer capacitor behavior and cycle stability. These

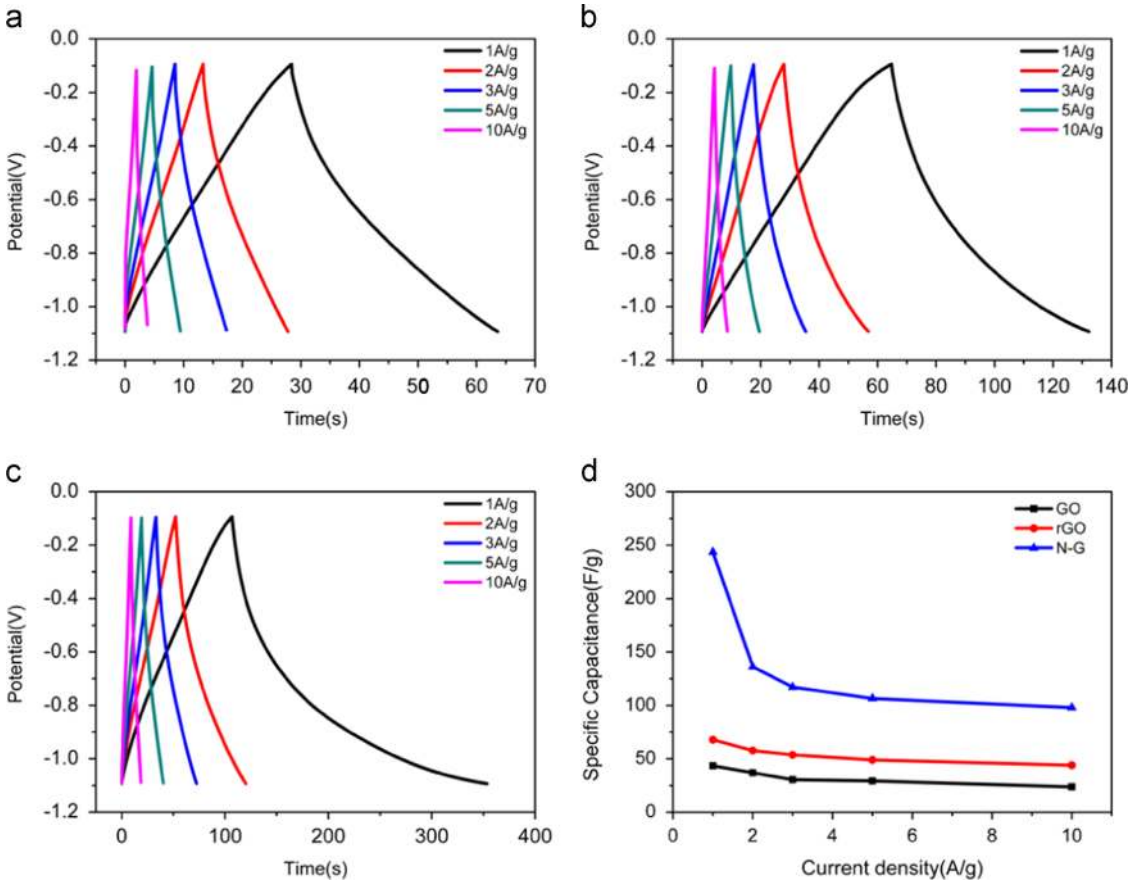

Fig. 6. Galvanostatic charge/discharge curves of samples. (a) GO, (b) rGO, (c) N-G; (d) Specific capacitances of GO, rGO and N-G at different current densities.

results reveal that the graphite electrodes possess excellent cyclic performance, and this is the main reason for their widely applications on supercapacitors. In addition, it could be observed that the capacitance decreased as the current density increasing. This is attributed to that the high current density accelerated the charge/discharge rate, and the ions in electrolyte were not able to diffuse completely into graphene layers and less electrode surface was utilized, which results in a low specific capacitance [21].

Fig. 6(d) illustrates the specific capacitance of three electrodes at different current densities. The specific capacitance (C) was calculated according to the equation $C = \frac{I\Delta t}{m\Delta V}$ where I is the constant current, m is the mass of active materials, Δt is the discharging time corresponding to the voltage change ΔV [22]. Compared with GO and rGO, the N-G electrode possessed the highest specific capacitance at the same current density. For example, the maximum capacitance (C) of the N-G electrode reached up to 243.5 F/g at 1 A/g, while GO was 43.5 F/g and rGO was 67.9 F/g. The reasons were the same as discussed above, i.e., porous microstructure was advantageous for the infiltration of electrolyte, and also contributed to the formation of electric double layer capacitor; the electron mobility improved after the reduction, which enhances the electron transport on the surface of electrodes, and insertion of N atoms changed the electronic structure of graphene.

3.7. Electrochemical impedance spectroscopy

Nyquist plots were used to analyze the electrochemical impedance spectroscopy (EIS) data and presented with the equivalent circuit inset, as shown in Fig. 7. Three electrodes all exhibited typical AC impedance characteristics of supercapacitors [21,25]. In the high frequency region (Fig. 7 inset), there gives two messages: 1) the real axis intercept represents a combined resistance (R_s) containing intrinsic resistance of electrode materials, ionic resistance of electrolyte and contact resistance between the electrode and current collector; 2) the radius of semicircle is indicative of the electrode conductivity and the charge-transfer resistance (R_{ct}) of electrode materials. The EIS plots exhibited identical R_s for N-G about 1.95 Ω, which was larger than that of GO (1.29 Ω) and rGO (1.76 Ω). And the fitted value of R_{ct} obtained for GO, rGO and N-G was 2.04 Ω, 0.23 Ω and 1.08 Ω, respectively. It may be due to the formation of defects on the surface during N-G preparation by using a hydrothermal process. In the intermediate frequency region, the slope of 45° portion of the curves was the Warburg resistance, which represents the ion diffusion/transport in the electrolyte. In the low frequency region the capacitive behavior of the N-G electrode performed on the curve. The curve was slightly bended, but overall exhibited a good capacitive performance.

As have discussed above, due to N doping the electrochemical properties of N-doped graphene changed greatly, which resulted in a much higher specific capacitance (243.5 F/g) than GO and rGO. In addition, the N-G electrode possessed

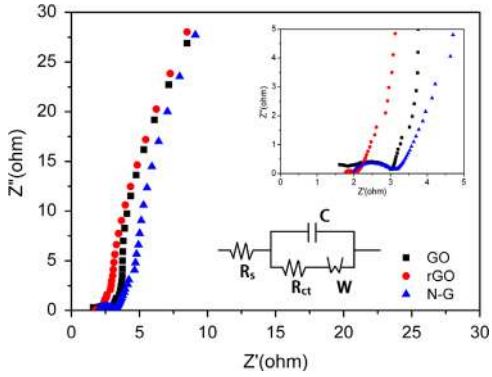

Fig. 7. EIS plots of GO, rGO and N-G (inset shows the electrochemical equivalent circuit).

an excellent capacitive performance. These experimental results demonstrate that N-doped graphene is an ideal electrode material for supercapacitors.

4. Conclusions

Due to a unique microstructure and excellent properties, graphene exhibits an enormous potential applications for energy storage devices. The present work reveals that, though graphene possesses superior and stable electrochemical properties, its different microstructures still exhibit great influences on the electrochemical properties. Therefore, it is very important to select the right and effective graphene-based electrode materials during practical applications. We propose that the N-doped graphene is an ideal electrode material for supercapacitors due to its best supercapacitance performance.

Acknowledgments

This work was supported by the National Natural Science Foundation of China (Nos. 11174227 and J1210061), National Key Technology R&D Program of the Hubei Province of China (No. 2013BHE012), Special Fund for the Development of Strategic Emerging Industries of Shenzhen City of China (No. JCYJ20140419141154246).

Reference

[1] M. Winter, R.J. Brodd, Chem. Rev. 104 (2004) 4245–4270.
[2] A.S. Aricò, P. Bruce, B. Scrosati, J.M. Tarascon, W.V. Schalkwijk, Nat. Mater. 4 (2005) 366–377.
[3] J.R. Miller, P. Simon, Science 321 (2008) 651–652.
[4] A.G. Pandolfo, A.F. Hollenkamp, J. Power Sources 157 (2006) 11–27.
[5] P. Simon, Y. Gogotsi, Nat. Mater. 7 (2008) 845–854.
[6] L.L. Zhang, X.S. Zhao, Chem. Soc. Rev. 38 (2009) 2520–2531.
[7] H. Jiang, P.S. Lee, C.Z. Li, Energy Environ. Sci. 6 (2013) 41–53.
[8] V. Singh, D. Joung, L. Zhai, S. Das, S.I. Khondaker, S. Seal, Prog. Mater. Sci. 56 (2011) 1178–1271.
[9] M. Pumera, Energy Environ. Sci. 4 (2011) 668–674.
[10] Y. Huang, J.J. Liang, Y.S. Chen, Small 8 (2012) 1805–1834.
[11] X.W. Yang, C. Cheng, Y.F. Wang, L. Qiu, D. Li, Science 341 (2013) 534–537.
[12] X.J. Liu, X. Qi, Z. Zhang, L. Ren, G.L. Hao, Y.D. Liu, Y. Wang, K. Huang, J. Lo, Z.Y. Huang, J.X. Zhong, RSC Adv. 4 (2014) 13673–13679.
[13] S.R.C. Vivekchand, C.S. Rout, K.S. Subrahmanyam, A. Govindaraj, C.N. R. Rao, J. Chem. Sci. 120 (2008) 9–13.
[14] M.D. Stoller, S. Park, Y.W. Zhu, J. An, R.S. Ruoff, Nano Lett. 8 (2008) 3498–3502.
[15] Y. Chen, X. Zhang, D.C. Zhang, P. Yu, Y.W. Ma, Carbon 49 (2011) 573–580.
[16] H.M. Jeong, J.W. Lee, W.H. Shin, Y.J. Choi, H.J. Shin, J.K. Kang, J. W. Choi, Nano Lett. 11 (2011) 2472–2477.
[17] W.S. Hummers, R.E. Offeman, J. Am. Chem. Soc. 80 (1958) 1339.
[18] H.B. Wang, T. Maiyalagan, X. Wang, ACS Catal. 2 (2012) 781–794.
[19] L.M. Liao, P.F. Fang, C.X. Pan, J. Nanosci. Nanotechnol. 11 (2011) 1060–1067.
[20] Y.P. Zhang, B. Cao, B. Zhang, X. Qi, C.X. Pan, Thin Solid Films 520 (2012) 6850–6855.
[21] B.E. Conway, Kluwer Academic/Plenum Publishers, New York, 1999.
[22] S.L. Zhang, N. Pan, Adv. Energy Mater. 5 (2015) 1401401.
[23] D.L. Li, C.Z. Yu, M.S. Wang, Y.P. Zhang, C.X. Pan, RSC Adv. 4 (2014) 55394–55399.
[24] B. Biel, X. Blase, F. Triozon, S. Roche, Phys. Rev. Lett. 102 (2009) 096803.
[25] D.Y. Qu, J. Power Sources 109 (2002) 403–411.